UNIVERSITY of York

This is a repository copy of *A high-resolution picture of kinship practices in an Early Neolithic tomb*.

White Rose Research Online URL for this paper:
https://eprints.whiterose.ac.uk/185799/

Version: Accepted Version

Article:

Fowler, Chris, Olalde, Inigo, Cummings, Vicki et al. (7 more authors) (2022) A high-resolution picture of kinship practices in an Early Neolithic tomb. Nature. pp. 584-587. ISSN 0028-0836

https://doi.org/10.1038/s41586-021-04241-4

Reuse
Items deposited in White Rose Research Online are protected by copyright, with all rights reserved unless indicated otherwise. They may be downloaded and/or printed for private study, or other acts as permitted by national copyright laws. The publisher or other rights holders may allow further reproduction and re-use of the full text version. This is indicated by the licence information on the White Rose Research Online record for the item.

Takedown
If you consider content in White Rose Research Online to be in breach of UK law, please notify us by emailing eprints@whiterose.ac.uk including the URL of the record and the reason for the withdrawal request.

White Rose
university consortium
Universities of Leeds, Sheffield & York

eprints@whiterose.ac.uk
https://eprints.whiterose.ac.uk/

A high-resolution picture of kinship practices in an Early Neolithic tomb

Chris Fowler[1*†], Iñigo Olalde[2,3,4*†], Vicki Cummings[5], Ian Armit[6], Lindsey Büster[6], Sarah Cuthbert[7], Nadin Rohland[2,8], Olivia Cheronet[9], Ron Pinhasi[9†] and David Reich[2,8,10,11†]

[1]School of History, Classics and Archaeology, Newcastle University, Newcastle upon Tyne NE1 7RU, UK.
[2]Department of Genetics, Harvard Medical School, Boston, Massachusetts 02115, USA.
[3]BIOMICs Research Group, University of the Basque Country UPV/EHU, 01006 Vitoria-Gasteiz, Spain.
[4]Ikerbasque – Basque Foundation of Science, 48009 Bilbao, Spain.
[5]School of Natural Sciences, University of Central Lancashire, Preston, Lancashire PR1 2HE, UK.
[6]Department of Archaeology, University of York, York YO1 7EP, UK.
[7]Department of Archaeology, University of Exeter, EX4 4QE.
[8]Broad Institute of MIT and Harvard, Cambridge, MA 02142, USA.
[9]Department of Evolutionary Anthropology, University of Vienna, 1090 Vienna, Austria.
[10]Department of Human Evolutionary Biology, Harvard University, Cambridge, MA 02138.
[11]Howard Hughes Medical Institute, Boston, MA 02115, USA

* These authors contributed equally to this work.

† To whom correspondence should be addressed: chris.fowler@newcastle.ac.uk (C.F.); inigo.olalde@gmail.com (I.O.); ron.pinhasi@univie.ac.at (R.P); reich@genetics.med.harvard.edu (D.R.)

To explore kinship practices at chambered tombs in Early Neolithic Britain, we combined archaeological and genetic analyses of 35 individuals who lived about 5,700 years ago and were entombed at Hazleton North long cairn[1]. Twenty-seven are part of the first extended pedigree reconstructed from ancient DNA, a five-generation family whose many interrelationships provide statistical power to document kinship practices that were invisible without direct genetic data. Patrilineal descent was key in determining who was buried in the tomb, as all 15 inter-generational transmissions were through men. The presence of women who had reproduced with lineage men and the absence of adult lineage daughters suggests virilocal burial and female exogamy. We demonstrate that one male progenitor reproduced with four women: the descendants of two of those women were buried in the same half of the tomb over all generations. This suggests that maternal sub-lineages were grouped into branches whose distinctiveness was recognized during the tomb's construction. Four males descended from non-lineage fathers and mothers who also reproduced with lineage males, suggesting that some men adopted their reproductive partners' children by other males into their patriline. Eight individuals were not close biological relatives of the main lineage, raising the possibility that kinship also encompassed social bonds independent of biological relatedness.

41 Genome-wide ancient DNA analysis has emerged as a transformative tool for understanding how
42 past people related to each other and to people today. To date, these studies have mostly focused
43 on changes in deep ancestry proportions over time which can be accurately characterized with
44 only a handful of individuals per population[2,3]. Recently, ancient DNA has been increasingly
45 applied to provide insight into social phenomena[4–7]. Yet, while more than a thousand pairs of
46 first- to fourth-degree relatives have been documented in the ancient DNA literature, there have
47 been almost no multi-generational families[5,7] where the exact relationships of all the individuals
48 have been uniquely characterized. In studies of Neolithic chambered tombs in Britain and
49 Ireland, relatedness patterns documented to date include cases of first- or second- degree relative
50 pairs within or across tombs[8], persistence of particular Y-chromosome lineages in the same
51 tombs[8]; two brothers in the same chamber in England[9], and an absence of biological kin within
52 the third degree among 11 and 15 sampled individuals at two tombs in Ireland[4]. Our genome-
53 wide data on 36 individuals from the same tomb and reconstruction of a five-generation family
54 including 27 individuals which we co-analyse with contextual archaeological information thus
55 offers an unprecedented opportunity to understand social relations within the communities that
56 built and used these tombs. Such comprehensive reconstructions not only provide insight into the
57 genealogical aspects of kinship in past societies, but can also be used to identify kinship practices
58 that extend beyond genealogical descent. Anthropological studies have made it clear that
59 kinship—the relationships of family connection and belonging that play a central role in
60 organizing societies—varies dramatically across cultures. Biological relatedness may be of
61 greater or lesser importance in determining kinship; kin need not be biological relatives (or even
62 human), and child rearing is not always centered on the relationship between biological father
63 and mother[10–12]. Funerary practices often play an important role in the social negotiation of
64 connections and divisions between kin, and here we use this insight, along with the ability of
65 ancient DNA to document relatedness, to provide a window into the role of biology in
66 determining kinship among people who buried their dead in Neolithic chambered tombs.

67 Hazleton North, Gloucestershire, an Early Neolithic Cotswold-Severn chambered long cairn,
68 contained well-preserved human remains and was excavated in its entirety[1]. The tomb was
69 constructed in the thirty-seventh century BC[13], at least a hundred years after cattle and cereal
70 cultivation had been introduced to Britain along with the construction of megalithic
71 monuments[14]; prior to that, the overwhelming majority of the biological ancestors of those buried
72 at Hazleton North lived in continental Europe[2,3]. There are many other long cairns or long
73 barrows in the region, at least nine of which share with Hazleton North a bilateral arrangement of
74 chambers, although no two sites are identical and others have different chamber arrangements.
75 Hazleton North incorporates two opposed L-shaped chambered areas mirrored around the 'spine'
76 of the cairn; these roofed chambered areas were flanked by rectangular cells of masonry on
77 either side of the axial line and the whole cairn was enclosed by a retaining wall[1] (Fig. 1a). The
78 two chambered areas, north and south, each had three compartments: a chamber (innermost), a
79 passage, and an entrance (Fig. 1b and Extended Data Fig.1). Osteological analysis has identified
80 a minimum of 41 individuals within the tomb, including 22 adults[15,16]. The treatment of human
81 remains differs somewhat between the north and south chambers (Supplementary Information

82 Section 1): bones from more than five individuals in the north chambered area had been gnawed
83 by scavengers[15] suggesting exposure prior to deposition (Extended Data Fig.2); cremated
84 remains from three individuals were placed in the north entrance (one infant, one child and one
85 adult); and the remains in the south chambered area were more commingled and dispersed
86 among neighbouring compartments than in the north. The individuals buried at Hazleton North
87 exhibit a similar range of pathologies as those from contemporary tombs in southern Britain,
88 such as osteoarthritis and conditions suggesting nutritional stress in childhood[15] (such as cribra
89 orbitalia) (Supplementary Information section 1). Isotopic analysis indicates a diet rich in animal
90 proteins[17] while proteomic analysis confirms this included dairy products[18], which is also typical
91 for the region. Bayesian modelling of 44 radiocarbon dates suggested that the monument was
92 built over the course of a decade between 3,695–3,650 BC, with the stonework of the north
93 passage collapsing and sealing off the north chamber c. 3,660–3,630 BC, and the deposition of
94 the individuals in this study probably ceasing around 3,620 BC[13]. A study of strontium and
95 oxygen stable isotopes on teeth suggested that most of the 22 individuals sampled had spent
96 some of their childhood on geology at least 40 km away[19]. Here we interpret new ancient DNA
97 data alongside the archaeological evidence to reconstruct kinship practices among the
98 community who buried their dead at Hazleton North.

99 To generate ancient DNA data, we obtained powder from 74 samples, largely petrous bones and
100 teeth. We extracted DNA, generated double- and single-stranded libraries, enriched for
101 molecules overlapping approximately 1.2 million polymorphic positions in the nuclear human
102 genome as well as mitochondrial DNA, and sequenced these libraries (Methods). We obtained
103 data passing standard metrics for DNA authenticity for 156 libraries deriving from 66 samples
104 (Supplementary Table 1). After detecting samples that derived from the same individual and
105 merging the data, we had genome-wide data from 35 distinct individuals (Extended Data Table
106 1) with median coverage of 2.9-fold (range of 0.018 – 9.75-fold; Supplementary Table 1).

107 We estimated mismatch rates on the autosomes (Supplementary Tables 4, 5) for each pair of
108 individuals, randomly sampling one DNA sequence at each position on chromosomes 1–22, and
109 computed relatedness coefficients r (Supplementary Table 5, Methods). We also determined the
110 type of first-degree relationships based on uniparental markers (mtDNA and Y-chromosome)
111 (Supplementary Table 1) and based on the spatial pattern of mismatches along the chromosomes
112 (Supplementary Tables 5, 6 and Extended Data Fig. 3). We manually built family trees
113 (Supplementary Information Section 2; Fig. 1c and Extended Data Fig. 4) consistent with the
114 pairwise genetic degrees of relatedness (Extended Data Fig. 2); maternal (mtDNA) and paternal
115 (Y-chromosome) haplogroups; genetic sex (Supplementary Table 1); genetic inbreeding
116 (Extended Data Fig. 9) and age-at-death. After leveraging the distribution of recombination
117 events (Extended Data Fig. 5) we obtained a unique pedigree that fit the data for 27 individuals
118 (Fig. 1c). We determined that the inferred pedigree (Supplementary Information Section 2) was
119 entirely consistent with independent information from the X-chromosome (Extended Data Fig.
120 6a), the number of shared DNA segments (Extended Data Fig. 6b), and a different methodology
121 for kinship estimation (Extended Data Fig. 7). We introduce a nomenclature to refer to
122 individuals that first specifies location within the tomb (NC = North Chamber, NP = North

Passage, NE = North Entrance, SC = South Chamber, SP = South Passage, SE = South Entrance, U = Unsampled individual who may not even have been buried on the tomb but who we know must have existed based on their genetic relationship to other individuals, HN = uncertain location within the tomb), then specifies an arbitrary number to distinguish each individual from the others, and finally gives a letter to indicate their chromosomal sex. In this study we use "m/male/man" to indicate an individual with an X and a Y chromosome, and "f/female/woman" to indicate an individual with two X chromosomes, while recognizing that chromosomal sex is only one element in how sex and gender are contextually and culturally defined. In Extended Data Table 1, Supplementary Table 1 and 2 we provide translations between this nomenclature and genetic and osteological identifiers.

The reconstructed pedigree consists of a five-generation lineage descended from one male NC1m and four females with whom he reproduced (SC1f, NC2f, NC3f, and unsampled female U3f); also interred as part of this family are adult female reproductive partners of lineage males and male line descendants of these women and non-lineage males. The pedigree includes 27 individuals—three times as many individuals as the largest pedigrees reconstructed from ancient DNA[5,7]—and provides the first direct evidence that at least some Neolithic tombs were organized around kinship practices. Eight other individuals are not close biological relatives of the 27. The reconstructed pedigree includes a sufficiently rich network of relationships to identify kinship practices that would be invisible in smaller datasets (Extended Data Table 2 and Supplementary Table 7), while the inclusion in the tomb of eight individuals without evidence of close biological relationships or reproductive partnerships with others in the pedigree suggests either that kinship did not always depend on such relations or that kinship may not have been the only criterion for inclusion in the tomb throughout its use.

Mortuary treatment varied according to chromosomal sex in several ways. Firstly, each third-, fourth- or fifth-generation individual whose lineage we can trace through the second generation to the first is connected to NC1m entirely through males. Specifically, all 15 of the genealogical connections are through fathers (13 cases) or stepfathers (2 cases) (P=0.000061 from a two-side binomial test; Fig. 1c), providing the first direct evidence that patrilineal descent was a primary determinant of who was interred with whom in a Neolithic tomb. These observations are consistent with the inference that the persistence of rare Y-chromosome haplotypes over time among individuals from the same Neolithic tombs indicates patrilineal practices in these communities[4,8]. Secondly, 26 of 35 individuals with genetic data are biologically male (P=0.00599 from a two-sided binomial test), consistent with osteological[20] and genetic evidence[8] that chambered tombs in England and Ireland preferentially included biological males (for example, males outnumber females about 1.6 to 1 in Cotswold monuments)[20]. This suggests the remains of some women were treated in another way (e.g. exposure of remains to the elements or scattering of cremated remains away from the tomb). Thirdly, four women among those sampled had reproduced with lineage males, and their presence suggests virilocal burial, that is, burial with a male partner's lineage rather than their father's lineage. This, combined with the lack of adult lineage daughters among those sampled (0 adult daughters vs. 14 adult sons; P=0.00012 from a two-sided binomial test) and the presence of two lineage daughters who died in

164 childhood, suggests that women generally joined the lineage of their mate. While we do not
165 know the social or geographical distance involved in this patrilocal exogamy, the lack of long
166 runs of homozygosity which measures how closely a person's two parents are related to each
167 other for all but one individual indicates that inbreeding was effectively avoided (Extended Data
168 Fig. 9). These results show that patrilineal descent played an important role in shaping social
169 relations—a finding that provides some insight into the nature of the community at Hazleton
170 North (especially given the associations between patrilineal descent, virilocality, polygyny and
171 cattle husbandry documented in ethnographically diverse cultures[21])—but as we show below, the
172 spatial organization of the dead, and the inclusion of individuals who were not part of the
173 biological patriline, indicate that other considerations also had significant influence on burial
174 patterns.

175 We observe six instances of multiple reproductive partners (Fig. 1c), most notably male NC1m
176 who reproduced with four females. We cannot determine whether the latter was an instance of
177 serial monogamy or polygyny, and we cannot exclude the possibility of progeny from unions
178 that were not socially sanctioned in any of the six instances. Where men had multiple
179 reproductive partners those females were not closely related to one another (Extended Data Fig.
180 8). However, multiple reproductive partners of females were related in most cases, such as two
181 males in the patriline, NE2m and unsampled male U11m, who are inferred to be third-degree
182 relatives and who both produced offspring with female U6f. Another case is NC3f, who
183 reproduced with male NC1m and also with a different male who, although not descending from
184 NC1m, was likely his close relative. Such women may have formed important connections
185 between parallel lineages of related males.

186 Our data prove that the arrangement of chambers at this Neolithic tomb was centrally determined
187 by notions of kinship, a matter long debated for such monuments[22]. While determination of who
188 could be buried at Hazleton North was primarily patrilineal, we observe a significant spatial
189 patterning in the placement of individuals from different maternal sub-lineages, with all 12
190 individuals belonging to the sub-lineages of SC1f and U3f buried in the south, and 9 out 13
191 belonging to the sub-lineages of NC2f and NC3f buried in the north, including the first
192 generation mothers in the 3 out 4 cases where we have been able to locate them (P-value=0.0011
193 from a Fisher's Exact Test for a difference in the spatial placement of these four sub-lineages)
194 (Fig. 1b). We can therefore describe the pedigree as divided into a 'southern branch' and a
195 'northern branch', each consisting of two maternal lines. The fact that this duality is fundamental
196 to the tomb's architecture suggests that the builders anticipated this division. The collapse of
197 walling which blocked the junction of the north passage and entrance led to the deposition of
198 longer-lived second and third generation descendants of NC2f and NC3f outside the north
199 chamber, disrupting this duality and perhaps contributing to the abandonment of the tomb by the
200 northern branch (P-value=0.00408 from a one-sided Fisher's Exact Test for the individuals in
201 these two sub-lineages with a likely later date of death being buried outside the north chamber).
202 The fact that these branches were based on maternal descent provides evidence that the women
203 originating each sub-lineage were socially significant in the memories of these communities. The

interplay between patrilineal and maternal descent also has implications for interpreting the constitution of personhood and gender in this Neolithic community[23].

Our genetic analyses of individuals from Hazleton North reveal kinship practices that while consistent with patrilineality cannot all be explained by biological descent. Thus, NE1m, SE1m, and SE3m are not descendants of NC1m but instead are sons of women who had other children with him or his male-line genetic descendants; SP2m is the biological son of one of these individuals, SE1m. These four individuals represent cases of incorporation of males into a patriline when a man born into the lineage reproduced with their mothers: this could indicate adoptive kinship, although in two cases the fathers of these males were also third- or fourth-degree biological relatives of NC1m (Extended Data Fig. 8). Social fatherhood in this Neolithic community could be as important as biological fatherhood, a pattern observed ethnographically in societies such as the patrilineal and polygynous Nuer[24]. The presence of eight individuals who are not close biological relatives of any member of the lineage could be interpreted in several ways. Three were women; it is possible they were mates of lineage males but did not reproduce, or that we have not sampled their offspring (who likely would not have been buried in the tomb if they were grown adult daughters). Some or all of these eight may have been considered kin by association or co-residence, or by adoption, raising the possibility of a meaningful role for completely non-biological kinship within the community; however, it is possible that reasons other than kinship were a factor in their inclusion in the tomb and the presence of unrelated individuals is noted at tombs from the same period in Ireland[4]. Overall, however, it is clear that biological relationships and kin membership were critical to the placement of many of the dead in this tomb: two pairs of sub-lineages within a single patriline were core to the layout of the tomb, and most of those buried in the chambers were lineage members. We therefore infer that the patriline and maternal sub-lineages grounded in the first generation both played anchoring roles in how kinship was negotiated at a tomb designed to both bring together and sub-divide the community.

This analysis provides additional archaeological insights. Bayesian modelling of radiocarbon dates suggested Hazleton North was probably only in use for up to three generations, but the ancient DNA data document five generations in the southern chamber (Supplementary Information Section 4). Osteological identification of the minimum number of individuals in a tomb has the potential to greatly underestimate the numbers present[25], yet the 66 skeletal samples that produced genome-wide data included 31 cases of genetic duplicates despite selecting bones and teeth that were not attributed to the same individuals. This suggests that our sampling is well on its way to capturing a good fraction of the individuals whose remains were recovered from the tomb and adds strength to the osteological inference that Hazleton North accommodated tens rather than hundreds of individuals (Supplementary Information section 1). Approximately one hundred long cairns are known within 50km of Hazleton North; one just 80m away. Further excavation, radiocarbon dating and aDNA analyses are needed to assess how many of these exhibit similar contemporary kinship practices, but it is possible that a high proportion of the local contemporary kin groups built and used such tombs. We have too few measurements of

245 stable isotopes on the individuals we analysed to be able to study correlations to cross-geology
246 mobility[19] but isotopic analyses of additional individuals with genetic data could reveal
247 undetected patterns.

248 This study illustrates how ancient DNA analysis can be combined with archaeological evidence
249 to draw inferences about kinship practices invisible to other methods. In particular, our ability to
250 reconstruct a family tree spanning five continuous generations reveals the first direct evidence
251 for a central role for patrilineal descent in the Neolithic mortuary practices[5], the acceptance of
252 'step-sons' into the patriline, and a key role for maternal sub-lineages. Adoption or kinship by
253 association may also have played a role in the inclusion of biologically unrelated individuals.
254 Hazleton North cannot be considered a template for all Neolithic chambered tombs since the
255 layout of such monuments varied and kinship practices could have varied between (and within)
256 the different regions where such tombs were built[22]. Nonetheless, this analysis advances our
257 understanding of kinship and chambered tomb construction in Neolithic Britain. Future research
258 carrying out similar studies in additional tombs both in a Neolithic context in northern Europe
259 and in other cultural contexts has the potential to test alternative theories of kinship in past
260 societies.
261

262 **References**

263 1. Saville, A. *Hazleton North, Gloucestershire, 1979-82 : the excavation of a Neolithic long*
264 *cairn of the Cotswold-Severn group.* (Historic Buildings & Monuments Commission for
265 England, 1990).

266 2. Brace, S. *et al.* Ancient genomes indicate population replacement in Early Neolithic
267 Britain. *Nat. Ecol. Evol.* **3**, 765–771 (2019).

268 3. Olalde, I. *et al.* The Beaker phenomenon and the genomic transformation of northwest
269 Europe. *Nature* **555**, 190–196 (2018).

270 4. Cassidy, L. M. *et al.* A dynastic elite in monumental Neolithic society. **582**, (2020).

271 5. Mittnik, A. *et al.* Kinship-based social inequality in Bronze Age Europe. *Science* **366**,
272 731–734 (2019).

273 6. Yaka, R. *et al.* Variable kinship patterns in Neolithic Anatolia revealed by ancient
274 genomes. *Curr. Biol.* **31**, 2455-2468.e18 (2021).

275 7. Amorim, C. E. G. *et al.* Understanding 6th-Century Barbarian Social Organization and
276 Migration through Paleogenomics. *Nat. Commun.* **9**, (2018).

277 8. Sánchez-Quinto, F. *et al.* Megalithic tombs in western and northern Neolithic Europe were
278 linked to a kindred society. *Proc. Natl. Acad. Sci. U. S. A.* **116**, 9469–9474 (2019).

279 9. Scheib, C. L. *et al.* East Anglian early Neolithic monument burial linked to contemporary
280 Megaliths. *Ann. Hum. Biol.* **46**, 145–149 (2019).

281 10. Schneider, D. M. *A critique of the study of kinship*. (Ann Arbor : University of Michigan
282 Press, 1984).

283 11. Carsten, J. *After Kinship*. (Cambridge University Press, 2003).
284 doi:10.1017/CBO9780511800382

285 12. Brück, J. Ancient DNA, kinship and relational identities in Bronze Age Britain. *Antiquity*
286 **95**, 228–237 (2021).

287 13. Meadows, J., Barclay, A. & Bayliss, A. A short passage of time: The dating of the
288 hazleton long cairn revisited. *Cambridge Archaeol. J.* **17**, 45–64 (2007).

289 14. Rowley-Conwy, P. & Legge, T. Subsistence practices in western and northern Europe. In
290 *The Oxford Handbook of Neolithic Europe* (eds. Fowler, C., Hofmann, D. & Harding, J.)
291 429-446. (Oxford University Press, 2015).

292 15. Cuthbert, G. S. Enriching the neolithic : The forgotten people of the barrows. (University
293 o, 2018).

294 16. Rogers, J. *et al.* The human skeletal material. In *Hazleton North: The excavation of a*
295 *Neolithic long cairn of the Cotswold-Severn group* 182–198 (Liverpool University Press,
296 1990).

297 17. Hedges, R., Saville, A. & O’Connell, T. Characterizing the diet of individuals at the
298 Neolithic chambered tomb of Hazleton North, Gloucestershire, England, using stable
299 isotopic analysis. *Archaeometry* **50**, 114–128 (2008).

300 18. Charlton, S. *et al.* New insights into Neolithic milk consumption through proteomic
301 analysis of dental calculus. *Archaeol. Anthropol. Sci.* **11**, 6183–6196 (2019).

302 19. Neil, S., Evans, J., Montgomery, J. & Scarre, C. Isotopic evidence for residential mobility
303 of farming communities during the transition to agriculture in Britain. *R. Soc. Open Sci.* **3**,
304 (2016).

305 20. Smith, M. & Brickley, M. *People of the Long Barrows: Life, Death and Burial in Earlier*
306 *Neolithic Britain*. (The History Press, 2009).

307 21. Surowiec, A., Snyder, K. T. & Creanza, N. A worldwide view of matriliny: Using cross-
308 cultural analyses to shed light on human kinship systems. *Philos. Trans. R. Soc. B Biol.*
309 *Sci.* **374**, (2019).

310 22. Fowler, C. Social arrangements: kinship, descent and affinity in the mortuary architecture
311 of Early Neolithic Britain and Ireland. *Archaeol. Dialogues (In Press*, 2021).

312 23. Robb, J. & Harris, O. J. T. Becoming gendered in european prehistory: Was neolithic
313 gender fundamentally different? *Am. Antiq.* **83**, 128–147 (2018).

314 24. Stone, L. & King, D. E. *Kinship and Gender: An Introduction.* (Routledge, 2018).

315 25. Robb, J. What can we really say about skeletal part representation, MNI and funerary
316 ritual? A simulation approach. *J. Archaeol. Sci. Reports* **10**, 684–692 (2016).
317

318 **Fig. 1. The Hazleton North pedigree in the context of the physical structure of the tomb. a,**
319 Plan of Hazleton North showing the north and south chambered areas in the cairn (grey).
320 Adapted from[1]. **b**, Burial locations for individuals, with squares for males and circles for
321 females. Individuals are coloured according to the female sub-lineage they belong to. The
322 relative position of each individual within each compartment does not reflect the exact location
323 in which the corpse or remains were placed. **c**, Reconstruction of the pedigree, using the same
324 colour scheme and indicating the locations of individuals in the tomb, osteological information
325 including age estimates, and different mitochondrial DNA haplogroups as small circles with
326 different colours. Individuals with a dotted outline are unsampled (U) and their existence is
327 inferred. Pink, blue and orange dotted lines indicate likely second-, third- and fourth-degree
328 relationships, respectively. Marks at the top corners of individuals indicate how many
329 genealogical connections linking individuals in the third through fifth generations to male NC1m
330 traverse through that individual (in blue, connections through step-fathers).

331 # Methods
332

333 **Sampling and ancient DNA data generation**

334 We obtained permission from the Corinium Museum to sample 8 postcranial bones, 17 petrous
335 bones and 49 teeth from Hazleton North. Processing was carried out in dedicated clean rooms.
336 DNA was extracted from using an automated protocol with silica coated magnetic beads and
337 'Dabney binding buffer'[26]. DNA extracts equivalent to between 6 and 8 mg of powder were
338 converted into either single-stranded or double stranded libraries (Supplementary Table 1)
339 following automated library preparation. For some samples we built multiple libraries. USER
340 treatment was applied before single-stranded library preparation[27] and partial UDG treatment
341 before double-stranded library preparation[28]. Amplified libraries were enriched using two rounds
342 of consecutive hybridization capture enrichment ('1240k' strategy[29,30]) targeting 1,233,013 SNPs
343 and the mitochondrial genome or, 'Twist Ancient DNA' (Supplementary Table 1), a custom
344 probe panel synthesized by Twist Biosciences. This custom panel targets the very same
345 1,233,013 SNPs as well as additional SNPs and tiling regions (Twist probes targeting the
346 mitochondrial genome were spiked in) and was performed for only one round of enrichment
347 using reagents and buffers provided by Twist Biosciences. Captured libraries were sequenced
348 either on an Illumina NextSeq500 instrument with 2x76 cycles (2x7 cycles for the indices) or on
349 an Illumina HiSeq X10 with 2x101 cycles (2x7 for the indices) (Supplementary Table 1). For
350 this study, we restricted all our analysis to the 1,233,013 SNPs in common between '1240k' and
351 'Twist Ancient DNA' and the mitochondrial genome.

352 Following the same procedure as in Olalde *et al.* 2019[31], we trimmed adapter sequences, merged
353 paired-end sequences, aligned to both the human reference genome (hg19) and the mitochondrial
354 genome (RSRS) using BWA v0.6.1[32], and removed PCR duplicate sequences. The
355 computational pipelines are available on github (https://github.com/DReichLab/ADNA-Tools,
356 https://github.com/DReichLab/adna-workflow).

357 We evaluated ancient DNA (aDNA) authenticity using several criteria:

358 -A rate of cytosine deamination at the terminal nucleotide above 3%.

359 -A ratio of Y to combined X+Y chromosome sequences below 0.03 or above 0.35. Intermediate
360 values are indicative of the presence of DNA from two individuals of different sex.

361 -For males with sufficient coverage, an X-chromosome contamination estimate[33] below 5%.

362 -An upper bound rate for the 95% confidence interval for the rate to the consensus mitochondrial
363 sequence that exceeds 95%, as computed using *contamMix-1.0.10*[34].

364 Out of a total of 74 samples, 8 did not have any library passing these criteria and were discarded,
365 keeping 156 libraries from 66 samples for further analysis (Supplementary Table 1). We retained
366 for analysis one sample (I30332) with 42,000 SNPs recovered that did not have enough data to
367 test for mitochondrial or X-chromosome contamination. Given that it did not display evidence of

contamination according to the other two authenticity criteria, we decided to include this sample in the kinship analyses but to be cautious in the interpretation of results.

Genetic sex, mitochondrial and Y-chromosome haplogroup determination

To determine genetic sex, we looked for the presence or absence of Y-chromosome by computing the ratio of the number of Y-chromosomal 1240k positions with available data divided by the number of X- and Y-chromosomal 1240k positions with available data. Individuals with a ratio >0.35 were considered genetic males and individuals with a ratio<0.03 were considered genetic females (Supplementary Table 1). To check for sex-chromosome aneuploidies, we computed the mean coverage on X- and Y-chromosomal 1240k positions, and normalised these values by the autosomal coverage on 1240k positions for each individual. We did not find any evidence for sex-chromosome aneuploidies in any individual.

To determine mitochondrial haplogroups (Supplementary Table 1), we constructed a consensus sequence with *samtools* and *bcftools*[32], restricting to sequences with mapping quality >30 and base quality >30. We then called haplogroups with *Haplogrep2*[35].

We determined Y-chromosome haplogroups (Supplementary Table 1) based on the nomenclature of the International Society of Genetic Genealogy (http://www.isogg.org) version 14.76 (25 April 2019), restricting to sequences with mapping quality ≥ 30 and bases with quality ≥ 30.

Biological kinship estimation

We estimated pairwise allelic mismatch rates in the autosomes[31,36,37] for each pair of libraries (n=156) deriving from 66 different samples, randomly sampling one DNA sequence at each ‘1240k’ polymorphic position and masking the two terminal nucleotides of each sequence to reduce the effects of post-mortem deamination. We then computed relatedness coefficients *r* for each pair (Supplementary Table 4):

$$r = 1 - (2*(x-(b/2))/b)$$

with *x* being the mismatch rate of the pair under analysis and *b* the mismatch rate expected for two unrelated individuals from Neolithic Britain (0.2504; see Supplementary Information Section 2.2). We also computed 95% confidence intervals using block jackknife standard errors over 5 Megabase (Mb) blocks[38].

A total of 105 pairs of libraries stemming from 44 pairs of samples had relatedness coefficients larger than 0.85, indicating that they share their entire genome and that they derived from the same individual. To increase resolution in the kinship analysis, we merged the data from samples deriving from the same individual and from libraries deriving from the same sample, keeping 35 unique individuals for further analysis. We gave a unique identifier to each of these 35 individuals (Supplementary Table 1) based on their burial location and genetic sex (e.g., NC1m = male individual 1 from the north chamber)

403 We recomputed the mismatch rates and relatedness coefficients *r* on the merged dataset and
404 annotated degrees of relationship (Supplementary Table 5 and Extended Data Fig. 2). Following
405 a similar approach as in Monroy Kuhn *et al.* 2018[39], we used cutoffs lying halfway between the
406 expected relatedness coefficients for different degrees of genetic relationships: 1 for identical
407 twins or samples deriving from the same individuals, 0.5 for first-degree relationships (parent-
408 offspring and siblings), 0.25 for second-degree relationships (grandparent-grandchild,
409 uncle/aunt-nephew/niece, half-siblings, double cousins), 0.125 for third-degree relatives (first
410 cousins, great-grandparent-great-grandchild, half uncle/aunt-nephew/niece, etc) and 0.0625 for
411 fourth-degree relationships.

412 Additionally, we determined the type of relationship (siblings or parent-offspring) connecting
413 first-degree relatives based on uniparental markers (mtDNA and Y-chromosome) and the DNA
414 sharing along the chromosomes. To analyse DNA sharing patterns along the chromosomes, we
415 computed allelic mismatch rates patterns across sliding windows of 20 Mb, moving by 1 Mb
416 each step (Supplementary Table 6), and visually identified the presence (indicative of a sibling
417 relationship) or absence (indicative of a parent-offspring relationship) of regions with zero or
418 two chromosomes sharing for each first-degree relative pair with sufficient coverage. We
419 illustrate this approach in Extended Data Fig. 3a and annotate the type of relationship for each
420 first-degree pair (Supplementary Table 5).

421 **Family tree reconstruction**

422 We attempted to reconstruct the family tree relating 27 close biological relatives using the
423 pairwise degrees of genetic relatedness (Extended Data Fig. 2) through a process of triangulation
424 that allowed us to discard most tree topologies relating these individuals (Supplementary
425 Information Section 2.3). To aid this process, we also incorporated information regarding:

426 - The types of first-degree relationships (Supplementary Table 5).

427 - The mtDNA and Y-chromosome lineages transmitted through maternal and paternal lines
428 (Supplementary Table 1).

429 - Genetic sex (Supplementary Table 1).

430 - Presence or absence of runs of homozygosity (ROH) indicative of inbreeding (Extended Data
431 Fig. 9b).

432 - Age-at-death as determined through osteological analysis (Supplementary Table 1).

433 After this procedure, we kept two possible tree topologies differing on whether NC1m is the
434 father (Fig. 1c) or the son of SC3m (Extended Data Fig. 4). To disambiguate between these two
435 scenarios, we studied the co-localization of break points of shared DNA segments between
436 individual SC3m and each of his second-degree relatives NC4m, NE2m, SC2m and SP1m
437 (Supplementary Information Section 2.4; Extended Data Fig. 5). This allowed us to obtain a
438 unique family pedigree relating most of the Hazleton North individuals (Fig. 1c).

439 **Testing the validity of the proposed family tree**

440 We validated the family tree in Fig 1c using three independent lines of evidence (Supplementary
441 Information Section 2.5):

442 **-**We computed pairwise mismatch rates and relatedness coefficients on the X-chromosome
443 (Supplementary Table 5) following the same formula: $r = 1 - (2*(x-(b/2))/b)$. For male-male
444 comparisons, we adjusted the formula as follows to account for the fact that males have only one
445 X-chromosome: $r = 1 - (x/b)$. We plotted relatedness coefficients in the X-chromosome for first
446 and second-degree pairs (Extended Data Fig. 6a), grouping these pairs based on whether they are
447 expected to share X-chromosome DNA according to the tree structure proposed in Fig. 1c. We
448 found that X-chromosome sharing patterns perfectly fit the proposed tree structure.

449 **-**For each first- or second-degree pair with more than 100,000 overlapping SNPs, we computed
450 allelic mismatch rate values across sliding windows of 20 Mb, moving by 1 Mb each step
451 (Supplementary Table 6). We plotted these values along the chromosomes and visually identified
452 contiguous regions where the allelic mismatch rate is consistent with one shared chromosome
453 (Extended Data Fig. 3b). We annotated in Supplementary Table 5 the number of such segments
454 identified for each first and second-degree relative pair. We next plotted the number of IBD
455 segments for first- and second-degree relationships (Extended Data Fig. 6b), again grouping the
456 pairs according to their type of relationship in the proposed tree (Fig. 1c). We recovered the
457 expected pattern[40,41] of a higher number of IBD segments in avuncular and maternal half-sibling
458 pairs as compared to grandparent-grandchild and paternal half-sibling pairs, adding further
459 support to the proposed tree structure.

460 **-**We replicated our results using the software *NgsRelate* v.2[42] that uses genotype likelihoods and
461 population allele frequencies to estimate Cotterman coefficients k0, k1 and k2, which correspond
462 to the probability of sharing 0, 1 and 2 alleles in identity by descent. From these coefficients, the
463 software computes the Theta coefficient (θ) which is equivalent to the relatedness coefficient r.
464 To run *NgsRelate*, we first created genotype likelihoods directly from the bam alignment files
465 using ANGSD v0.923[33]. We included Hazleton North individuals as well as the set of 53
466 Neolithic individuals from other sites in Britain. We then ran *NgsRelate* providing as input the
467 genotype likelihood file and allele frequencies estimated only on the Neolithic set from Britain,
468 to avoid possible bias in allele frequencies stemming from the presence of a high number of
469 closely related individuals at Hazleton North. We observed a strong correlation between both
470 methodologies (Extended Data Fig 7)

471 **Principal component analysis (PCA)**

472 To obtain an overview of the ancestry of the Hazleton North individuals, we ran a principal
473 component analysis using the 'smartpca' program in EIGENSOFT[43]. We merged the genomic
474 data from the Hazleton North individuals with other ancient Neolithic and Bronze Age
475 individuals from Britain and Ireland reported in previous publications[2–4,8,9,44], as well as with
476 1109 present-day West Eurasian individuals genotyped on the Affymetrix Human Origins

477 Array[43,45,46], restricting to 591,642 SNPs that overlap between the 1240k capture and the Human
478 Origins Array. We projected ancient individuals onto the components computed on present-day
479 individuals with lsqproject:YES and shrinkmode:YES, and plotted the first two principal
480 components (Extended Data Fig. 9a). The Hazleton individuals form a homogeneous cluster
481 within the genomic diversity of contemporaneous Neolithic individuals from England, Scotland
482 and Ireland, indicating that they derived from a very similar pool of ancestors as other Neolithic
483 groups across Britain. We do not detect individuals shifted towards smaller values on PC1 that
484 would suggest recent admixture with Mesolithic hunter-gatherers.

485 **Genetic inbreeding analysis**

486 To study the presence of inbreeding in the Hazleton North group, we use the software *hapROH*[47]
487 that detects runs of homozygosity in ancient individuals. Runs of homozygosity are regions of an
488 individual's genome where the maternal and paternal chromosomes are identical because they
489 derive from a recent common ancestor. The number and length of these segments in a given
490 individual inform about the degree of biological relationship between the parents. We ran
491 *hapROH* using standard parameters on the Hazleton individuals with data for more than 400,000
492 SNPs covered (Supplementary Table 1 and Extended Data Fig. 9b). The software also computes
493 the ROH expected for offspring of close relatives in outbred populations, and for individuals
494 from populations with small effective population size[47]. The lack of long ROH in all but one
495 individual (Extended Data Fig. 9b) indicates that the Hazleton community effectively avoided
496 reproductive unions between close relatives. Only one individual (SE6f) had a long ROH of 31
497 cM, which could be compatible with offspring of second or third cousins. This individual does
498 not belong to the family pedigree.

499 **Data availability**

500 The aligned sequences are available through the European Nucleotide Archive, accession
501 PRJEB46958; the genotype dataset is available as Supplementary Data file.

502

503 **Additional references**

504 26. Rohland, N., Glocke, I., Aximu-Petri, A. & Meyer, M. Extraction of highly degraded
505 DNA from ancient bones, teeth and sediments for high-throughput sequencing. *Nat.*
506 *Protoc.* **13**, 2447–2461 (2018).

507 27. Gansauge, M. T., Aximu-Petri, A., Nagel, S. & Meyer, M. Manual and automated
508 preparation of single-stranded DNA libraries for the sequencing of DNA from ancient
509 biological remains and other sources of highly degraded DNA. *Nat. Protoc.* **15**, 2279–
510 2300 (2020).

511 28. Rohland, N., Harney, E., Mallick, S., Nordenfelt, S. & Reich, D. Partial uracil – DNA –
512 glycosylase treatment for screening of ancient DNA. *Philos. Trans. R. Soc. London B* **370**,
513 (2015).

514 29. Fu, Q. *et al.* An early modern human from Romania with a recent Neanderthal ancestor.

515 *Nature* **524**, 216–219 (2015).

516 30. Fu, Q. *et al.* DNA analysis of an early modern human from Tianyuan Cave, China. *Proc.*
517 *Natl. Acad. Sci. U. S. A.* **110**, 2223–7 (2013).

518 31. Olalde, I. *et al.* The genomic history of the Iberian Peninsula over the past 8000 years.
519 *Science* **363**, 1230–1234 (2019).

520 32. Li, H. & Durbin, R. Fast and accurate short read alignment with Burrows–Wheeler
521 transform. *Bioinformatics* **25**, 1754–1760 (2009).

522 33. Korneliussen, T. S., Albrechtsen, A. & Nielsen, R. ANGSD : Analysis of Next Generation
523 Sequencing Data. *BMC Bioinformatics* **15**, 1–13 (2014).

524 34. Fu, Q. *et al.* A revised timescale for human evolution based on ancient mitochondrial
525 genomes. *Curr. Biol.* **23**, 553–9 (2013).

526 35. Weissensteiner, H. *et al.* HaploGrep 2: mitochondrial haplogroup classification in the era
527 of high-throughput sequencing. *Nucleic Acids Res.* **44**, W58-63 (2016).

528 36. Kennett, D. J. *et al.* Archaeogenomic evidence reveals prehistoric matrilineal dynasty.
529 *Nat. Commun.* **8**, 14115 (2017).

530 37. van de Loosdrecht, M. *et al.* Pleistocene North African genomes link Near Eastern and
531 sub-Saharan African human populations. *Science* **360**, 548–552 (2018).

532 38. Busing, F. M. T. A., Meijer, E. & Van Der Leeden, R. Delete- m Jackknife for Unequal m.
533 *Stat. Comput.* **9**, 3–8 (1999).

534 39. Monroy Kuhn, J. M., Jakobsson, M. & Günther, T. Estimating genetic kin relationships in
535 prehistoric populations. *PLoS One* **13**, 1–21 (2018).

536 40. Williams, C. *et al.* A rapid, accurate approach to inferring pedigrees in endogamous
537 populations. 1–27 (2020).

538 41. Kong, A. *et al.* Fine-scale recombination rate differences between sexes, populations and
539 individuals. *Nature* **467**, 1099–1103 (2010).

540 42. Hanghøj, K., Moltke, I., Andersen, P. A., Manica, A. & Korneliussen, T. S. Fast and
541 accurate relatedness estimation from high-throughput sequencing data in the presence of
542 inbreeding. *Gigascience* **8**, 1–9 (2019).

543 43. Patterson, N. *et al.* Ancient admixture in human history. *Genetics* **192**, 1065–93 (2012).

544 44. Cassidy, L. M. *et al.* Neolithic and Bronze Age migration to Ireland and establishment of
545 the insular Atlantic genome. *Proc. Natl. Acad. Sci. U. S. A.* **113**, 1–6 (2016).

546 45. Lazaridis, I. *et al.* Ancient human genomes suggest three ancestral populations for
547 present-day Europeans. *Nature* **513**, 409–413 (2014).

548 46. Biagini, S. A. *et al.* People from Ibiza: an unexpected isolate in the Western
549 Mediterranean. *Eur. J. Hum. Genet.* 941–951 (2019).

550 47. Ringbauer, H., Novembre, J. & Steinrücken, M. Parental relatedness through time
551 revealed by runs of homozygosity in ancient DNA. *Nat. Commun.* **12**, 5425 (2021)
552

553 **Acknowledgments** This work was supported by NIH grant GM100233, by the Allen Discovery
554 Center program, a Paul G. Allen Frontiers Group advised program of the Paul G. Allen Family
555 Foundation, by John Templeton Foundation grant 61220, by a gift from Jean-François Clin, and
556 by the Howard Hughes Medical Institute. I.O. is supported by a Ramón y Cajal grant from
557 Ministerio de Ciencia e Innovación, Spanish Government (RYC2019-027909-I). We thank
558 James Harris and Alison Brookes at the Corinium Museum for providing permission to sample
559 skeletal material from Hazleton North; Tom Booth, Alissa Mittnik, Harald Ringbauer and
560 Alasdair Whittle for valuable discussions; and Nicole Adamski, Rebecca Bernardos, Guillerma
561 Bravo, Kimberly Callan, Elizabeth Curtis, Ann Marie Lawson, Matthew Mah, Swapan Mallick,
562 Adam Micco, Lijun Qiu, Kristin Stewardson, Anna Wagner, J. Noah Workman, and Fatma
563 Zalzala for laboratory and bioinformatic work.

564 **Author contributions** N.R., O.C., S.C., R.P., and D.R. performed or supervised laboratory
565 work. C.F., V.C., I.A., L.B. and S.C. assembled or contextualized archaeological material. C.F.
566 and I.O. analyzed data. C.F., I.O., and D.R. wrote the manuscript, and C.F., I.O., and S.C. wrote
567 the supplement.

568 **Competing interests** The authors declare no competing interests.

569

570 **Additional Information** is available for this paper at https:XX.

571 **Extended Data Table 1. Key details for sampled individuals**. The individual code consists of
572 the location of the remains, then a number for the individual within that location, and finally their
573 sex. For those with an osteological code, this value is provided in parentheses. Full details,
574 including bone element numbers, radiocarbon dates and stable isotope data are provided in
575 Supplementary Table 1. Fr. = fracture; Gn. = gnawed by canids; AMTL = ante-mortem tooth
576 loss; DA = dental abscess; DISH = Diffuse Idiopathic Skeletal Hyperostosis CO = cribra
577 orbitalia; OA = osteoarthritis; OD = osteochondritis dissecans; PH = porotic hyperostosis; SA =
578 septic arthritis.

579

580 **Extended Data Table 2. Statistically significant patterns in genetic data.** Two-sided binomial
581 tests for rows 1–3, Fisher's exact tests for row 4 (two-sided) and row 5 (one-sided). See
582 Supplementary Section 3 and Supplementary Table 3 for details.

583

584 **Extended Data Figure 1. The Hazleton North chambered tomb. a,** Distribution of human
585 remains in both chambers (adapted from[1]). **b**, Right humerus from Individual C showing helical
586 fracture (red arrow), tooth marks (yellow arrow) and gnawed proximal and distal ends (white
587 arrows).

588

589 **Extended Data Figure 2. Degrees of biological relatedness among individuals at Hazleton**
590 **North** (Supplementary Information section 2.2). Pairs with fewer than 15,000 overlapping SNPs
591 are indicated with an asterisk.

592

593 **Extended Data Figure 3. Using allelic mismatch rates patterns along the chromosomes to**
594 **differentiate types of relationships for individuals sharing the same amount of DNA. a**,
595 Differentiating between parent-offspring and sibling relationships. Allelic mismatch rate values
596 across sliding windows of 20 Mb, moving by 1 Mb each step. As an example, we show values at
597 chromosome 17 and include for reference a comparison between two unrelated Neolithic
598 individuals from Britain (in brown), and a comparison between one individual and himself (in
599 purple) to show how mismatch rates behave when two chromosomes are shared. The mismatch
600 rate pattern for SP1m-SC1f is compatible with one chromosome shared along the entire
601 chromosome 14 (in fact, along all autosomal chromosomes (Supplementary Table 6)), indicating
602 a parent-offspring relationship. In contrast, the NC7f-SP3m comparison shows regions on
603 chromosome 17 where no chromosome is shared (~65–70 Mb), other regions where two
604 chromosomes are shared (~0–25 Mb) and other regions where one chromosome is shared (~25–
605 60 Mb), compatible with a sibling relationship. **b,** Comparing DNA sharing patterns between
606 SC9f and her paternal grandparents. We show mismatch rate values at chromosome 2 and
607 include for reference a parent-offspring comparison (SE1m-SP2m; in blue) to show how
608 mismatch rates behave when one chromosome is shared. Two recombination events (one at ~145
609 Mb and other at ~220 Mb) in SC9f's father's gamete result in SC9f's sharing one chromosome
610 with SC3m from the start of the chromosome to ~145 Mb, one chromosome with SC4f from 145
611 to 220 Mb and one chromosome with SC3m from 220 Mb to the end of the chromosome. This
612 pattern of sharing one chromosome with either SC3m or SC4f at every location of the genome is

613 characteristic of comparisons between a grandchild and his/her two grandparents and is also
614 observed in the other autosomal chromosomes.

615

616 **Extended Data Figure 4**. **Alternative family tree fitting all the genetic evidence except the**
617 **IBD breakpoints co-localization analysis** (Supplementary Section 2.4, Extended Data Figure
618 5). Individuals are coloured according to the female sub-lineage they belong to (NC1m and
619 NC5m do not belong to any of the four major sub-lineages and are thus given a different color).

620

621 **Extended Data Figure 5**. **Using co-localization of IBD breakpoints to disambiguate between**
622 **family tree in Fig. 1c and family tree in Extended Data Fig. 4**. **a,** We show mismatch rate
623 values across sliding windows of 20 Mb on chromosome 3, moving by 1 Mb each step, for
624 comparisons between SC3m and his four second-degree relatives. Recombination events on
625 chromosome 3 needed to explain the observed mismatch rate patterns under **b,** the scenario of
626 tree in Fig 1c. where 4 recombination events are required or **c,** the scenario of the tree in
627 Extended Data Fig.4 where 10 recombination events are required including the extremely
628 implausible occurrence of two recombination events at the same genomic locations in four
629 different gametes.

630

631 **Extended Data Figure 6**. **Testing the validity of the family pedigree in Fig. 1c using X-**
632 **chromosome relatedness and number of shared IBD segments. a,** Relatedness coefficients in
633 the X-chromosome for first and second degree relationships with more than 300 overlapping
634 SNPs. For each comparison, expected values according to the type of relation in the family tree
635 in Fig. 1c are shown in grey boxes. Bars represent 95% confidence intervals. **b,** Number of
636 shared IBD segments for first- and second-degree relationships. Pairs are grouped according to
637 their type of relation in the family tree in Fig. 1c.

638

639 **Extended Data Figure 7**. **Testing the consistency of the kinship results using *NgsRelate*[42]**. **a**,
640 Correlation between the relatedness coefficient r and the Theta coefficient computed with
641 *NgsRelate*, restricting to comparisons with more than 15,000 overlapping SNPs. **b**, Cotterman
642 coefficients k0 and k2 for first and second degree relationships, as computed with *NgsRelate*.

643

644 **Extended Data Figure 8**. **Comparing autosomal relatedness between reproductive partners,**
645 **different male reproductive partners of a female and different female reproductive**
646 **partners of a male.** To estimate relatedness coefficients between unsampled and sampled male
647 reproductive partners of a female, we doubled the relatedness coefficient obtained between the
648 son of the unsampled male and the sampled male, to account for the fact that a son is one degree
649 of relationship further away from their father's relatives as compared to his father. Bars represent
650 95% confidence intervals.

651

652 **Extended Data Figure 9**. **Principal Component Analysis and inbreeding analysis. a,**
653 Principal component analysis of Hazleton North individuals and other ancient individuals from
654 Britain and Ireland. Ancient individuals were projected onto the principal components computed
655 on a set of present-day West Eurasians genotyped on the Human Origins Array (not shown in the
656 figure). Individuals with fewer than 15,000 SNPs on the Human Origins dataset were excluded
657 for this analysis. **b,** Runs of homozygosity (ROH) in different length categories for the Hazleton
658 North individuals with higher than 400,000 SNPs covered. ROH were computed using
659 *hapROH*[47]. On the right, we plot the expected ROH length distribution for the offspring of
660 closely related parents in outbred populations and for individuals from populations with small
661 effective population size[47].

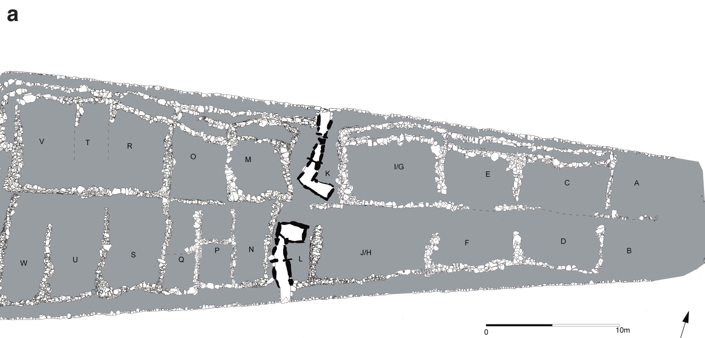

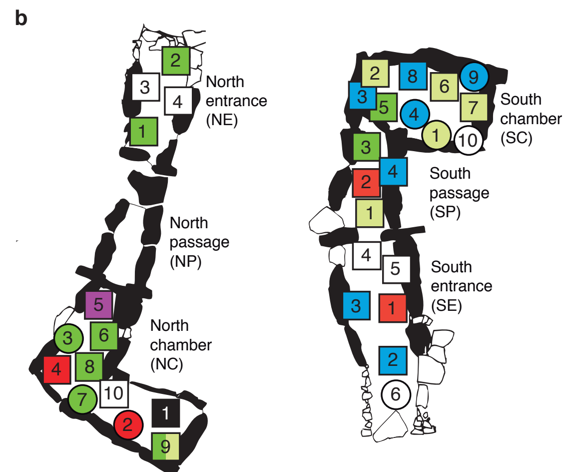

c

Gen 1
U1m
17-25 NC2f (C)
U2m
40+ NC3f (F)
Adult NC1m
Adult SC1f
U3f

Gen 2
Adult SE1m
U4f
17-25 NC4m
33-60 NE1m (2)
U5f
23-57 NE2m (A)
U6f
U7f
Adult SC2m
Adult SP1m (ii)
U8f
U9m
3-4 NC5m (G)
45+ SC3m (ix)
48-56 SC4f
U10m

Gen 3
25-35 SP2m (vi)
2-3 NC6m (H)
9-15 SC5m (E)
Child NC7f
45+ SP3m
Infant NC8m
U11m
5-6 SC6m
Adult SC7m
U12f
U13m
Adult SE2m (v)
U14f
35-45 SE3m

Gen 4
Adult NC9m
U15f
U16m
25-35 SC8m
6-9 SC9f

Gen 5
Child SP4m (i)

Connection to NC1m
Female
Male
4-4 NC4m (G)
Age
Sample ID
Osteological individual
mtDNA lineage

Non-lineage
Adult NC10m
3-6 mts. NE3m (B)
c.40 NE4m (1)
23-35 SC10f (viii)
Adult SE4m (D)
Adult SE5m
Adult SE6f
HN1f